

# Fully Implicit Formulation and Its Solution for Rotor Dynamics by Using Differential Algebraic Equation (DAE) Solver and Partial Periodic Trimming Algorithm (PPTA)

Chang-Joo Kim\*, Chul Yong Yun, and Seok Choi

Rotorcraft Development Division, Korea Aerospace Research Institute,  
45 Eoeun-Dong, Yuseong-Gu, Daejeon, 305-333, South Korea

## Abstract

The implicit formulation of rotor dynamics and its application to helicopter flight mechanics have been presented. The generalized vector kinematics regarding the relative motion between coordinates were expressed as a unified matrix operation and applied to get an inertial velocity and acceleration at arbitrary blade span position. Based upon these results the rotor aeromechanic equations for blade flapping, blade lead-lag and rotor torque (engine dynamics) have been formulated as a fully implicit DAE (Differential Algebraic Equations) form. While most current formulations can evoke some doubt in its validity and its applicable range of flight envelope after simplification or ordering, it is easy to validate the present results and to re-drive the rotor aeromechanic equations for any rotor with arbitrary hinge geometry and hinge sequence.

For flight dynamic analysis, DAE based PPTA (Partial Periodic Trimming Algorithm) has been developed. The iterative update of PPTA always makes the initial conditions incompatible for DAE solver, which causes a numerical instability. By reducing the order of DAE solver at the initial stage of PPTA iteration DAE solver can be integrated into PPTA with good convergence characteristics. The present formulation and the DAE based PPTA are applied for Bo-105 helicopter and the results are compared with the results of AGARD GARTEUR AG06 to show its convergence characteristics and accuracy.

## Symbols

$C$	Hinge damping coefficient
$C_D$	Airfoil drag coefficient
$C_L$	Airfoil lift coefficients
$C_M$	Airfoil pitching moment coefficient
$e_x, e_y, e_z$	Unit vector in the direction of x, y and z
$F$	A coordinate system
$F^{Aero}$	Blade section aerodynamic forces
$I$	Identity matrix
$K$	Hinge spring coefficient

$l$	Hinge offset distance
$L$	Coordinate transform matrix
$m_b$	Blade mass per unit length
$M^{Aero}$	Blade section aerodynamic moments
$n_b$	Number of blade
$p, q, r$	Airframe angular velocity
$P$	Transformation matrix for periodicity
$Q$	Torque
$r, v, a$	Position, velocity and acceleration vector
$r_b$	Blade span position from outer hinge
$U_T, U_P$	Tangential and normal components of blade section velocity
$u, v, w$	Airframe velocity
$V_F$	Flight speed
$\beta$	Flapping angle
$\beta^{(j)}$	Flapping angle of blade j (j=1, 2, 3, 4)
$\delta$	Blade Pitch Control Input
$\varepsilon$	Small perturbation
$\phi, \theta, \psi$	Airframe roll, pitch and yaw angle
$\theta^A$	Blade pitch angle
$\Omega$	Rotor rotational speed
$\omega$	Angular velocity vector
$\tilde{\omega}$	Matrix expression of angular velocity If $\omega = [p, q, r]^T$

$$\tilde{\omega}(p, q, r) = \begin{bmatrix} 0 & -r & q \\ r & 0 & -p \\ -q & p & 0 \end{bmatrix}$$

$$= p\tilde{\omega}(1, 0, 0) + q\tilde{\omega}(0, 1, 0) + r\tilde{\omega}(0, 0, 1)$$

$$= pE_1 + qE_2 + rE_3$$

$\omega^P, \omega^C$	Predictor and corrector polynomials
$\psi_R$	Blade azimuth angle
$\lambda$	Non-dimensional inflow
$\zeta$	Lead-lag angle
$\zeta^{(j)}$	Lead-lag angle of blade j (j=1, 2, 3, 4)

## Subscripts

0, 1C, 1S	Collective, 1 <sup>st</sup> cos and 1 <sup>st</sup> sin harmonic components
TR	Tail rotor

## 1. Introduction

Rotorcraft flight dynamic modeling, applicable up to OFE (Operational Flight Envelope), generally needs the Level 2 rotor modeling, which requires (1) the numerical integration of rotor aerodynamic forces and moments along blade span, (2) the rotor dynamics for flap, lead-lag and torque (or engine dynamics), (3) the limited inclusion of blade elastic deformation (Ref 1, 2). Most formulations have been derived, based on one of following methods.

- (1) explicit formulation(Ref 3)
- (2) implicit formulation (Ref 4, 5, 6)
- (3) by using algebraic manipulator software

The derived equations are generally expressed in the form of DAE (Differential Algebraic Equation) like  $f(\dot{x}, x, u, t) = 0$ , where the state derivatives  $\dot{x}$  are implicitly included (Ref 7). Also the choice of adequate solver for DAE is not so simple. In case one of ODE solvers were used, the DAE form of equations should be inevitably converted into ODE form  $\dot{x} = g(x, u, t)$  by applying ordering scheme and it is difficult to define the applicable flight envelope because of the ignored higher order terms. Also if any components like main rotor inflow, tail rotor flapping and tail rotor inflow are modeled algebraically, the algebraic equation solver should be applied between each time integration steps. In case of DAE solver the same solution procedure can be simultaneously applied to both DAE and algebraic equations without any timing problems.

Recently R. Celi (Ref 8) has applied DAE solver to rotorcraft aeromechanic equations for trim analysis and flight simulation with two step trim routine. After main rotor partial trim was calculated, the unsteady aerodynamic forces and moments due to unsteady rotor motion have been considered to get a periodic trim response of fuselage (rigid body dynamics). He explained two step trim routine was required to get a periodic trim solution through time integration of flight dynamic equations. But in his paper there is no explanation why the efficient periodic trim algorithm (Ref 9, 10) was not used.

In this paper the rotor aeromechanic equations for flapping, lead-lag motion and torque dynamics have been derived in fully implicit DAE form with no ordering. It is easy to find any errors during derivation and easy to reuse or modify the derived equations for different rotor configuration (e.g. change in hinge configuration or addition of another hinge, etc.). To get an efficient periodic trim DAE solver has been integrated into PPTA (Partial Periodic Trimming Algorithm). The update of initial condition in PPTA supplies the incompatible initial condition to DAE solver, which can cause a numerical instability. This problem has been

overcome by simply adjusting the order of DAE solver. The present DAE based PPTA has been applied to Bo-105 helicopter to show the fast convergence in trim calculation. Also the effect of the size of time step, the number of blade span wise elements and the order of DAE solver on the periodic trim results has been investigated to recommend the analysis conditions for the accurate trim prediction and simulation. The average trim states calculated with DAE based PPTA have been correlated with the results of AGARD GARTEUR AG-06 (Ref 11).

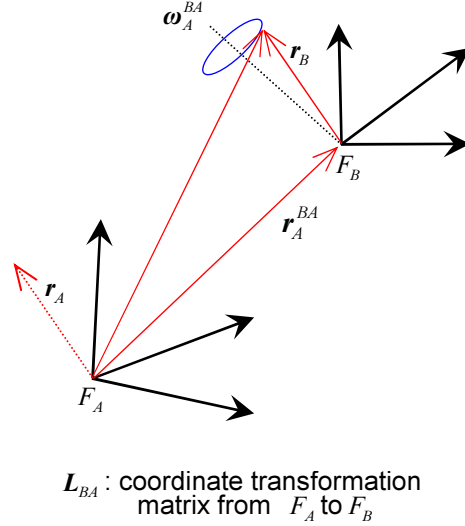


Fig. 1 Coordinates and Displacement Vectors

## 2. Vector Kinematics among Moving Coordinates

In this paper vector kinematics between coordinate systems have been derived by generalizing the approach of B. Etkin (Ref 12) and the same notational convention is used in the mathematical expressions.

### 2.1 Transformation of the derivative of a vector

An arbitrary vector  $r$  can be expressed in two different coordinates  $F_A$  and  $F_B$  which have relative motions as in Fig 1. If subscript  $A$  and  $B$  are used to identify the corresponding coordinate, the following relations are satisfied.

$$\begin{aligned} r_B &= L_{BA} r_A \\ r_A &= L_{AB} r_B \end{aligned} \quad (1)$$

Where  $L_{BA}$  denotes a coordinate transformation matrix from  $F_A$  to  $F_B$ .  $L_{AB}$  is its inverse. The vector  $r_A$  and  $r_B$  represent the displacement vector

$\mathbf{r}$  expressed as components in  $F_A$  and  $F_B$ , respectively. The following coordinate transform relations are satisfied.

$$\begin{aligned} \mathbf{L}_{BA}\mathbf{L}_{AB} &= \mathbf{I} \\ |\mathbf{L}_{BA}| &= |\mathbf{L}_{AB}| = 1 \\ \mathbf{L}_{BA}^{-1} &= \mathbf{L}_{AB} = \mathbf{L}_{BA}^T \end{aligned} \quad (2)$$

The derivatives of equation (1) is

$$\begin{aligned} \dot{\mathbf{r}}_B &= \dot{\mathbf{L}}_{BA}\mathbf{r}_A + \mathbf{L}_{BA}\dot{\mathbf{r}}_A \\ \dot{\mathbf{r}}_A &= \dot{\mathbf{L}}_{AB}\mathbf{r}_B + \mathbf{L}_{AB}\dot{\mathbf{r}}_B \end{aligned} \quad (3)$$

Let  $\mathbf{r}_B$  be an arbitrary constant vector in  $F_B$ , then its derivatives vector in  $F_A$  can be expressed as follow.

$$\dot{\mathbf{r}}_A = \tilde{\boldsymbol{\omega}}_A^{BA} \times \mathbf{r}_A = \tilde{\boldsymbol{\omega}}_A^{BA} \mathbf{r}_A \quad (4)$$

, where  $\tilde{\boldsymbol{\omega}}$  is matrix expression of angular velocity  $\boldsymbol{\omega}$  and the superscript  $BA$  denotes that it is a relative angular velocity of coordinate  $F_B$  with respect to  $F_A$ . The same notational convention is used throughout this paper. The differentiation of equation (1) gives an expression for the derivative of coordinate transformation matrix

$$\begin{aligned} \dot{\mathbf{r}}_A &= \dot{\mathbf{L}}_{AB}\mathbf{r}_B + \mathbf{L}_{AB}\dot{\mathbf{r}}_B = \dot{\mathbf{L}}_{AB}\mathbf{r}_B \\ \dot{\mathbf{r}}_B &= \dot{\mathbf{L}}_{BA}\mathbf{r}_A + \mathbf{L}_{BA}\dot{\mathbf{r}}_A = (\dot{\mathbf{L}}_{BA} + \mathbf{L}_{BA}\tilde{\boldsymbol{\omega}}_A^{BA})\mathbf{r}_A = 0 \end{aligned} \quad (5)$$

$$\begin{aligned} \dot{\mathbf{L}}_{AB} &= \tilde{\boldsymbol{\omega}}_A^{BA} \mathbf{L}_{AB} \\ \dot{\mathbf{L}}_{BA} &= -\mathbf{L}_{BA} \tilde{\boldsymbol{\omega}}_A^{BA} \end{aligned} \quad (6)$$

The relative angular velocities satisfy  $\tilde{\boldsymbol{\omega}}^{BA} = -\tilde{\boldsymbol{\omega}}^{AB}$ , which is independent to the specific coordinate ( $\tilde{\boldsymbol{\omega}}_A^{BA} = -\tilde{\boldsymbol{\omega}}_A^{AB}$ ,  $\tilde{\boldsymbol{\omega}}_B^{BA} = -\tilde{\boldsymbol{\omega}}_B^{AB}$ ). With the application of these relations to an arbitrary constant vector  $\mathbf{r}_A$  in  $F_A$ , the following coordinate transformation relations for angular velocity and angular acceleration between two coordinates can be obtained.

$$\tilde{\boldsymbol{\omega}}_A^{BA} = \mathbf{L}_{AB} \tilde{\boldsymbol{\omega}}_B^{BA} \mathbf{L}_{BA} \quad (7)$$

$$\tilde{\boldsymbol{\omega}}_A^{BA} = \mathbf{L}_{AB} \tilde{\boldsymbol{\omega}}_B^{BA} \mathbf{L}_{BA} \quad (8)$$

The transform of the derivative of a vector  $\mathbf{r}_A$  can be expressed as

$$\mathbf{L}_{BA}\dot{\mathbf{r}}_A = \dot{\mathbf{r}}_B + \tilde{\boldsymbol{\omega}}_B^{BA} \mathbf{r}_B \quad (9)$$

## 2.2 Velocity and acceleration in an arbitrary moving coordinates

To get the transformation relations when another coordinate are added, let's define three coordinates of an inertial coordinate  $F_I$  and two moving coordinates,  $F_A$  and  $F_B$ . Then following relations are satisfied.

$$\mathbf{L}_{BI} = \mathbf{L}_{BA} \mathbf{L}_{AI} \quad (10)$$

$$\mathbf{L}_{BI}^{-1} = \mathbf{L}_{BI}^T = \mathbf{L}_{IA} \mathbf{L}_{AB} = \mathbf{L}_{IB} \quad (11)$$

From time derivative of equation (10),

$$\tilde{\boldsymbol{\omega}}_B^{BI} = \tilde{\boldsymbol{\omega}}_B^{BA} + \mathbf{L}_{BA} \tilde{\boldsymbol{\omega}}_A^{AI} \mathbf{L}_{AB} \quad (12)$$

Also angular acceleration  $\ddot{\boldsymbol{\omega}}_B^{BI}$  can be expressed by differentiating equation (12).

$$\ddot{\boldsymbol{\omega}}_B^{BI} = \ddot{\boldsymbol{\omega}}_B^{BA} + \dot{\tilde{\boldsymbol{\omega}}}_B^{AI} - \tilde{\boldsymbol{\omega}}_B^{BA} \tilde{\boldsymbol{\omega}}_B^{AI} + \tilde{\boldsymbol{\omega}}_B^{AI} \tilde{\boldsymbol{\omega}}_B^{BA} \quad (13)$$

, where  $\tilde{\boldsymbol{\omega}}_B^{AI} = \mathbf{L}_{BA} \tilde{\boldsymbol{\omega}}_A^{AI} \mathbf{L}_{AB}$  and  $\dot{\tilde{\boldsymbol{\omega}}}_B^{AI} = \mathbf{L}_{BA} \dot{\tilde{\boldsymbol{\omega}}}_A^{AI} \mathbf{L}_{AB}$

The displacement vector and its 1<sup>st</sup> and 2<sup>nd</sup> derivatives can be derived by using the above transformation relations.

$$\mathbf{r}_I^{BI} = \mathbf{r}_I^{AI} + \mathbf{L}_{IA} \mathbf{r}_A^{BA}$$

$$\begin{aligned} \dot{\mathbf{r}}_I^{BI} &= \dot{\mathbf{r}}_I^{AI} + \dot{\mathbf{L}}_{IA} \mathbf{r}_A^{BA} + \mathbf{L}_{IA} \dot{\mathbf{r}}_A^{BA} \\ &= \dot{\mathbf{r}}_I^{AI} + \mathbf{L}_{IA} \dot{\mathbf{r}}_A^{BA} - \mathbf{L}_{IA} \tilde{\boldsymbol{\omega}}_A^{IA} \mathbf{r}_A^{BA} \\ &= \dot{\mathbf{r}}_I^{AI} + \mathbf{L}_{IA} \dot{\mathbf{r}}_A^{BA} + \mathbf{L}_{IA} \tilde{\boldsymbol{\omega}}_A^{AI} \mathbf{r}_A^{BA} \end{aligned}$$

$$\begin{aligned} \ddot{\mathbf{r}}_I^{BI} &= \ddot{\mathbf{r}}_I^{AI} + \mathbf{L}_{IA} \ddot{\mathbf{r}}_A^{BA} + 2\mathbf{L}_{IA} \tilde{\boldsymbol{\omega}}_A^{AI} \dot{\mathbf{r}}_A^{BA} \\ &\quad + \mathbf{L}_{IA} (\dot{\tilde{\boldsymbol{\omega}}}_A^{AI} + \tilde{\boldsymbol{\omega}}_A^{AI} \tilde{\boldsymbol{\omega}}_A^{AI}) \mathbf{r}_A^{BA} \end{aligned}$$

The vector components in  $F_A$  coordinate can be obtained by transforming with  $\mathbf{L}_{AI}$ .

$$\mathbf{r}_A^{BI} = \mathbf{L}_{AI} \mathbf{r}_I^{BI} = \mathbf{r}_A^{AI} + \mathbf{r}_A^{BA} \quad (14)$$

$$\dot{\mathbf{r}}_A^{BI} = \mathbf{L}_{AI} \dot{\mathbf{r}}_I^{BI} = \dot{\mathbf{r}}_A^{AI} + \dot{\mathbf{r}}_A^{BA} + \tilde{\boldsymbol{\omega}}_A^{AI} \mathbf{r}_A^{BA} \quad (15)$$

$$\begin{aligned} \ddot{\mathbf{r}}_A^{BI} &= \mathbf{L}_{AI} \ddot{\mathbf{r}}_I^{BI} = \ddot{\mathbf{r}}_A^{AI} + \ddot{\mathbf{r}}_A^{BA} + 2\tilde{\boldsymbol{\omega}}_A^{AI} \dot{\mathbf{r}}_A^{BA} \\ &\quad + (\dot{\tilde{\boldsymbol{\omega}}}_A^{AI} + \tilde{\boldsymbol{\omega}}_A^{AI} \tilde{\boldsymbol{\omega}}_A^{AI}) \mathbf{r}_A^{BA} \end{aligned} \quad (16)$$

## 3. Fully Implicit Formulation of Rotor Dynamics

Based upon the vector kinematics in section 2 the rotor aeromechanical equations for Level 2 modeling have been derived. To show the applicability and give a physical meaning, the formulation has been applied for an example rotor configuration defined in Fig. 2.

### 3.1 Sequential application of kinematical relation

In case multiple coordinates over three are required, above relations can be sequentially applied to get a linear velocity and linear acceleration at arbitrary position. The following is a brief description for the sequential process of derivation.

(1) The information about  $F_A$  (previously known)

$$\mathbf{L}_{AI}, \mathbf{r}_A^{AI}, \dot{\mathbf{r}}_A^{AI}, \ddot{\mathbf{r}}_A^{AI}, \tilde{\boldsymbol{\omega}}_A^{AI}, \dot{\tilde{\boldsymbol{\omega}}}_A^{AI}$$

(2) Define relative motions of new coordinate  $F_B$

$$\mathbf{r}_A^{BA}, \dot{\mathbf{r}}_A^{BA}, \ddot{\mathbf{r}}_A^{BA}$$

(3) Derivation of relative displacement, velocity and inertial acceleration at the origin of  $F_B$

$$\mathbf{r}_B^{BI}, \dot{\mathbf{r}}_B^{BI}, \ddot{\mathbf{r}}_B^{BI}$$

(4) If further coordinate transform is required, define

$$\mathbf{L}_{BA}, \tilde{\boldsymbol{\omega}}_A^{BA}, \dot{\tilde{\boldsymbol{\omega}}}_A^{BA}$$

(5) Repeat above processes as required.

### 3.2 Configuration of the example rotor system

The configuration of an example rotor system as in Fig 2 is selected because it enough covers the general configuration from the flight dynamic view points. Parameters defining the geometric character are summarized in Table 1. The related coordinates are identified with notation, major variables, coordinate transformation matrix, relative displacement vector and relative angular velocity vector.  $\mathbf{L}_1, \mathbf{L}_2, \mathbf{L}_3$  are the coordinate transformation matrices as defined in equation (17) and  $\mathbf{e}_x, \mathbf{e}_y, \mathbf{e}_z$  be the unit vectors in x, y, z direction, respectively

$$\mathbf{L}_1(x) = \begin{bmatrix} 1 & 0 & 0 \\ 0 & \cos x & \sin x \\ 0 & -\sin x & \cos x \end{bmatrix} \quad \mathbf{L}_2(y) = \begin{bmatrix} \cos y & 0 & -\sin y \\ 0 & 1 & 0 \\ \sin y & 0 & \cos y \end{bmatrix}$$

$$\mathbf{L}_3(z) = \begin{bmatrix} \cos z & \sin z & 0 \\ -\sin z & \cos z & 0 \\ 0 & 0 & 1 \end{bmatrix} \quad (17)$$

The direction of each coordinate axis can be easily identified. As an example, helicopter CG coordinate has x axis in forward direction, y-axis in starboard side and z axis in downward direction. The forward shaft tilt angle has the positive sign and the rotor azimuth angle is measured from the position when reference blade is directed to empennage.

For simplicity, the matrices related with the matrix expression of angular velocity are defined as

$$\mathbf{E}_1 = \tilde{\boldsymbol{\omega}}(1,0,0), \quad \mathbf{E}_2 = \tilde{\boldsymbol{\omega}}(0,1,0), \quad \mathbf{E}_3 = \tilde{\boldsymbol{\omega}}(0,0,1)$$

### 3.3 Linear velocity and linear acceleration at arbitrary blade span position

For flight dynamic analysis the velocity and acceleration of airframe are traditionally defined in airframe CG axis and can be defined as follow.

$$\dot{\mathbf{r}}_C^{CI} = \mathbf{v}_C^{CI} = \begin{bmatrix} u \\ v \\ w \end{bmatrix}, \quad \ddot{\mathbf{r}}_C^{CI} = \mathbf{a}_C^{CI} = \begin{bmatrix} \dot{u} - rv + qw \\ \dot{v} - pw + ru \\ \dot{w} - qu + pv \end{bmatrix}$$

$$\boldsymbol{\omega}_C^{CI} = \begin{bmatrix} p \\ q \\ r \end{bmatrix}, \quad \dot{\boldsymbol{\omega}}_C^{CI} = \begin{bmatrix} \dot{p} \\ \dot{q} \\ \dot{r} \end{bmatrix}$$

The sequential application of above kinematical relations from body C.G. coordinate  $F_C$  up to blade section coordinate  $F_T$  gives the following linear velocity  $\mathbf{v}_T^{GI}$  at blade section aerodynamic center and linear acceleration  $\mathbf{a}_T^{GI}$  at blade section C.G..

$$\mathbf{v}_T^{GI} = \mathbf{L}_{TR} \mathbf{v}_R^{RI} + \mathbf{L}_{TR} \tilde{\boldsymbol{\omega}}_R^{RI} \mathbf{d}_R - \dot{\beta} \mathbf{L}_{TF} \mathbf{E}_2 \mathbf{d}_F - \dot{\zeta} \mathbf{L}_{TL} \mathbf{E}_3 \mathbf{d}_L$$

$$\mathbf{a}_T^{GI} = \mathbf{L}_{TR} \mathbf{a}_R^{RI} + \mathbf{L}_{TR} (\dot{\tilde{\boldsymbol{\omega}}}_R^{RI} + \tilde{\boldsymbol{\omega}}_R^{RI} \tilde{\boldsymbol{\omega}}_R^{RI}) \mathbf{d}_R + \mathbf{L}_{TF} \dot{\beta} \mathbf{d}_F$$

$$+ \mathbf{L}_{TL} \dot{\zeta} \mathbf{d}_L + \mathbf{L}_{TA} \dot{\theta} \mathbf{d}_A + 2\dot{\zeta} \beta \mathbf{L}_{TF} \mathbf{E}_2 \mathbf{L}_{FL} \mathbf{E}_3 \mathbf{d}_L$$

$$- 2\dot{\theta} \beta \mathbf{L}_{TF} \mathbf{E}_2 \mathbf{L}_{FA} \mathbf{E}_1 \mathbf{d}_A - 2\dot{\theta} \dot{\zeta} \mathbf{L}_{TL} \mathbf{E}_3 \mathbf{L}_{LA} \mathbf{E}_1 \mathbf{d}_A$$

Where the coordinate transformation matrix can be calculated by the serial matrix product and as an example  $\mathbf{L}_{TR}$  has the following expression.

$$\mathbf{L}_{TR} = \mathbf{L}_{TA} \mathbf{L}_{AL} \mathbf{L}_{LF} \mathbf{L}_{FS} \mathbf{L}_{SP} \mathbf{L}_{PR}$$

The linear velocity, linear acceleration and angular velocity vectors represented in rotating hub coordinate  $F_R$ .

$$\mathbf{v}_R^{RI} = \mathbf{L}_{RC} (\mathbf{v}_C^{CI} + \tilde{\boldsymbol{\omega}}_C^{CI} \mathbf{r}_C^{HC})$$

$$\mathbf{a}_R^{RI} = \mathbf{L}_{RC} (\mathbf{a}_C^{CI} + \dot{\tilde{\boldsymbol{\omega}}}_C^{CI} \mathbf{r}_C^{HC} + \tilde{\boldsymbol{\omega}}_C^{CI} \tilde{\boldsymbol{\omega}}_C^{CI} \mathbf{r}_C^{HC})$$

$$\tilde{\boldsymbol{\omega}}_R^{RI} = \mathbf{L}_{RC} \tilde{\boldsymbol{\omega}}_C^{CI} \mathbf{L}_{CR} + \boldsymbol{\Omega} \mathbf{E}_3$$

The displacement vectors at each coordinates are;

$$\mathbf{d}_A = \mathbf{r}_A^{GA} = \mathbf{r}_B \mathbf{e}_X + l_{CA} \mathbf{L}_{AT} \mathbf{e}_Y$$

$$\mathbf{d}_L = \mathbf{r}_L^{GL} = (l_A + r_B \mathbf{L}_{LA}) \mathbf{e}_X + l_{CA} \mathbf{L}_{LT} \mathbf{e}_Y$$

$$\mathbf{d}_F = \mathbf{r}_F^{GF} = (l_L + l_A \mathbf{L}_{FL} + r_B \mathbf{L}_{FA}) \mathbf{e}_X + l_{CA} \mathbf{L}_{FT} \mathbf{e}_Y$$

$$\mathbf{d}_R = \mathbf{r}_R^{GR} = (l_p + l_S \mathbf{L}_{RP} + l_F \mathbf{L}_{RS} + l_L \mathbf{L}_{RF} + l_A \mathbf{L}_{RL} + r_B \mathbf{L}_{RA}) \mathbf{e}_X + l_{CA} \mathbf{L}_{RT} \mathbf{e}_Y$$

The angular acceleration terms due to flap, lead-lag and pitch control are as follow

$$\dot{\beta} = -\ddot{\beta} \mathbf{E}_2 - 2\dot{\beta} \mathbf{L}_{FR} \tilde{\boldsymbol{\omega}}_R^{RI} \mathbf{L}_{RF} \mathbf{E}_2 + \dot{\beta}^2 \mathbf{E}_2 \mathbf{E}_2$$

$$\dot{\zeta} = -\ddot{\zeta} \mathbf{E}_3 - 2\dot{\zeta} \mathbf{L}_{LR} \tilde{\boldsymbol{\omega}}_R^{RI} \mathbf{L}_{RL} \mathbf{E}_3 + \dot{\zeta}^2 \mathbf{E}_3 \mathbf{E}_3$$

$$\dot{\theta} = \ddot{\theta} \mathbf{E}_1 - 2\dot{\theta} \mathbf{L}_{AR} \tilde{\boldsymbol{\omega}}_R^{RI} \mathbf{L}_{RA} \mathbf{E}_1 + \dot{\theta}^2 \mathbf{E}_1 \mathbf{E}_1$$

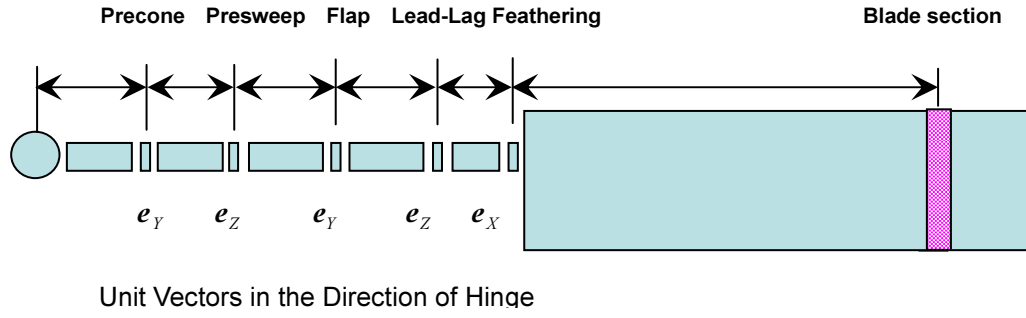


Fig. 2 Configuration of example rotor system

Table 1 Geometric definition of example rotor system

Coordinates System	Sym-bol	Main variables		Coordinate transform matrix	Relative position vector	Relative Angular velocity
Airframe CG	$C$					
Hub Fixed	$H$	Shaft tilt Position	$\gamma_S$ $x_H, y_H, z_H$	$L_{HC} = L_2(\pi - \gamma_S)$	$\mathbf{r}_C^{HC} = \begin{bmatrix} x_H \\ y_H \\ z_H \end{bmatrix}$	$\tilde{\omega}_C^{HC} = \mathbf{0}$
Rotating Hub	$R$	Azimuth angle	$\psi_R$	$L_{RH} = L_3(\psi_R)$	$\mathbf{r}_H^{RH} = \mathbf{0}$	$\tilde{\omega}_H^{RH} = \Omega \mathbf{E}_3$
Pre-cone	$P$	Pre-cone angle Offset distance	$\beta_P$ $l_P$	$L_{PR} = L_2(-\beta_P)$	$\mathbf{r}_R^{PR} = l_P \mathbf{e}_X$	$\tilde{\omega}_R^{PR} = \mathbf{0}$
Pre-sweep	$S$	Pre-sweep angle Offset distance	$\zeta_P$ $l_S$	$L_{SP} = L_3(-\zeta_P)$	$\mathbf{r}_P^{SP} = l_S \mathbf{e}_X$	$\tilde{\omega}_P^{SP} = \mathbf{0}$
Flap hinge	$F$	Flap angle Hinge offset	$\beta$ $l_F$	$L_{FS} = L_2(-\beta)$	$\mathbf{r}_S^{FS} = l_F \mathbf{e}_X$	$\tilde{\omega}_S^{FS} = -\dot{\beta} \mathbf{E}_3$
Lead-lag hinge	$L$	Lead-lag angle Hinge offset	$\zeta$ $l_L$	$L_{LF} = L_3(-\zeta)$	$\mathbf{r}_F^{LF} = l_L \mathbf{e}_X$	$\tilde{\omega}_F^{LF} = -\dot{\zeta} \mathbf{E}_3$
Feathering hinge	$A$	Pitch Angle Hinge offset	$\theta_A$ $l_A$	$L_{AL} = L_1(\theta_A)$	$\mathbf{r}_L^{AL} = l_A \mathbf{e}_X$	$\tilde{\omega}_L^{AL} = \dot{\theta} \mathbf{E}_1$
Blade section	$T$	Twist and torsion Blade span Section CG/ AC	$\theta_T$ $r_B$ $l_{CA}$	$L_{TA} = L_1(-\theta_T)$	$\mathbf{r}_A^{TA} = r_B \mathbf{e}_X$ $\mathbf{r}_T^{GT} = l_{CA} \mathbf{e}_Y$	

Table 2 Definition of Symbols

Symbols	Flap	Lead-Lag	Torque
$\Phi$	$\beta$	$\zeta$	$\Omega$
$\bar{H}$	$F$	$L$	$R$
$L_{\bar{H}T}$	$L_{FT}$	$L_{LT}$	$L_{RT}$
$e_{\bar{H}}$	$-e_Y$	$-e_Z$	$e_Z$
$I_A$	0	0	$I_{DRV}$
$Q_A$	0	0	$Q_{Engine}$
$C_\Phi$	$C_\beta$	$C_\zeta$	0
$K_\Phi$	$K_\beta$	$K_\zeta$	0

Note 1)  $I_{DRV}$  denotes the equivalent moment of inertia due to gear box, engine, gas generator, drive shaft and etc. except the contribution due to rotor blade and hinges which is included in the integral part of rotor equation.

Note 2)  $Q_{Engine}$  denotes engine torque transferred to rotor to overcome rotor torque.

### 3.4 Equations for rotor dynamics

The general form of hinge moment equation can be represented as the follow equation and for flap, lead-lag and torque, the corresponding notations are given in Table. 2.

$$\left[ \int \left( \bar{r}_{\bar{H}}^{GH} \times L_{\bar{H}T} \left\{ dF_T^{Aero} - m_b \left( a_T^{GI} - g_T^{GI} \right) dr_b \right\} + L_{\bar{H}T} dM_T^{Aero} \right) \cdot e_{\bar{H}} - I_A \ddot{\Phi} - C_\Phi \dot{\Phi} - K_\Phi \Phi + Q_A = 0 \right]$$

,where

$\bar{H}$	Notation for general hinge coordinates
$\bar{r}_{\bar{H}}^{GH}$	Displacement vector from hinge to blade section coordinate (CG or AC)
$e_{\bar{H}}$	Unit vector in the direction of hinge
$\Phi$	Hinge angular displacement
$I_A$	Moment of Inertia due to accessory subsystem except rotor blade
$Q_A$	Torque source except rotor blade

The equations by using fully implicit formulation for rotor dynamics have the following forms.

#### Flap equation for individual blade

$$\int \left[ m_b \bar{r}_F^{GF} \times L_{FT} (a_T^{GI} - g_T^{GI}) \cdot e_Y dr_b - C_\beta \dot{\beta} - K_\beta \beta \right] = \int \left( \bar{r}_F^{GF} \times L_{FL} dF_L^{aero} + L_{FL} dM_L^{aero} \right) \cdot e_Y \quad (18)$$

#### Lead-lag equation for individual blade

$$\int \left[ m_b \bar{r}_L^{GL} \times L_{LT} (a_T^{GI} - g_T^{GI}) \right] \cdot e_Z dr_b - C_\zeta \dot{\zeta} - K_\zeta \zeta = \int \left( \bar{r}_L^{GL} \times dF_L^{aero} + dM_L^{aero} \right) \cdot e_Z \quad (19)$$

#### Torque equations for rotor system

$$\sum \int \left[ m_b \bar{r}_R^{GR} \times L_{RT} (a_T^{GI} - g_T^{GI}) \right] \cdot e_Z dr_b + I_{DRV} \ddot{\Omega} = \sum \int \left( \bar{r}_R^{GR} \times L_{RL} dF_L^{aero} + L_{RL} dM_L^{aero} \right) \cdot e_Z + Q_{Engine} \quad (20)$$

### 3.5 Aerodynamic forces, moments and gravitational forces at blade section

The velocity vector to calculate aerodynamic forces and moments can be represented as components in lead-lag axis for the rotor configuration in Fig.2. If wind components due to turbulence and induced inflow are included, the velocity components and the angle of attack in blade section can be easily defined.

$$\begin{aligned} v_L^{GI} &= L_{LT} v_T^{GI} \\ v_L^{aero} &= v_L^{GI} - v_L^{tur} - v_L^{ind} = [U_R \quad U_T \quad U_P]^T \end{aligned}$$

$$\begin{aligned} \phi &= \tan^{-1}(U_P / U_T) \\ \alpha &= \theta - \phi = v_L^{GI} = \theta - \tan^{-1}(U_P / U_T) \end{aligned}$$

The aerodynamic forces and moments are represented as follow.

$$dF_L^{Aero} = \begin{bmatrix} 0 \\ -dL \sin \phi - dD \cos \phi \\ dL \cos \phi - dD \sin \phi \end{bmatrix}, \quad dM_L^{Aero} = \begin{bmatrix} dM \\ 0 \\ 0 \end{bmatrix}$$

, where

$$\begin{aligned} dL &= \frac{1}{2} C_L \rho V^2 c dr_b & dD &= \frac{1}{2} C_D \rho V^2 c dr_b \\ dM &= \frac{1}{2} C_M \rho V^2 c^2 dr_b & V^2 &= U_T^2 + U_P^2 \end{aligned}$$

The gravitation acceleration at blade section is a simple coordinate transform of body components.

$$\begin{aligned} g_T^{GI} &= L_{TA} L_{AL} L_{LF} L_{FS} L_{SP} L_{PR} L_{RH} L_{HC} g_C^{CI} \\ g_C^{CI} &= g [-\sin \theta \quad \cos \theta \sin \phi \quad \cos \theta \cos \phi]^T \end{aligned}$$

### 4 Flight Dynamic Equations for Trim Analysis

The flight dynamic equations including the rotor dynamics can be represented as a system of general nonlinear DAE. If rigid body states  $x_R$ , flap  $x_F$ , lead-lag  $x_L$ , inflow  $x_I$ , tail rotor states  $x_T$ , and rotor speed  $x_\Omega$  are considered, they have the

following form.

$$f(\dot{\mathbf{x}}, \mathbf{x}, \mathbf{u}, t) = [f_R, f_F, f_L, f_I, f_T, f_Q]^T = 0 \quad (21)$$

$$\mathbf{x} = [\mathbf{x}_R \quad \mathbf{x}_F \quad \mathbf{x}_L \quad \mathbf{x}_I \quad \mathbf{x}_T \quad \mathbf{x}_Q]^T$$

$$\mathbf{x}_R = [u, v, w, p, q, r, \phi, \theta, \psi]^T$$

$$\mathbf{x}_F = [\dot{\beta}^{(1)}, \dot{\beta}^{(2)}, \dot{\beta}^{(3)}, \dot{\beta}^{(4)}, \beta^{(1)}, \beta^{(2)}, \beta^{(3)}, \beta^{(4)}]^T$$

$$\mathbf{x}_L = [\dot{\zeta}^{(1)}, \dot{\zeta}^{(2)}, \dot{\zeta}^{(3)}, \dot{\zeta}^{(4)}, \zeta^{(1)}, \zeta^{(2)}, \zeta^{(3)}, \zeta^{(4)}]^T$$

$$\mathbf{x}_I = [\lambda_0, \lambda_{1C}, \lambda_{1S}]^T$$

$$\mathbf{x}_T = [\beta_{TR0}, \beta_{TR1C}, \beta_{TR1S}, \lambda_{TR0}]^T$$

$$\mathbf{x}_Q = \Omega$$

And the trim conditions applicable for both straight flight and steady turning flight are

$$\mathbf{f}_{TRM} = [f_{TRM1}, f_{TRM1}, f_{TRM1}, f_{TRM1}]^T = \mathbf{0}$$

, where

$$f_{TRM1} = V_F \sin \gamma_C - u \sin \phi \cos \theta + w \cos \phi \cos \theta$$

$$f_{TRM2} = V_F^2 - u^2 - v^2 - w^2$$

$$f_{TRM3} = v - V_F \sin \beta$$

$$f_{TRM4} = \dot{\psi} - (q \sin \phi + r \cos \phi) / \cos \theta$$

$$\dot{\psi} = \pm \frac{g}{V_F} \sqrt{\frac{n_T^2}{\cos \gamma_C^2} - 1.0}$$

$V_F, \gamma_C, \beta$ , and  $n_T$  denote flight speed, flight path angle, side slip and normal load factor, respectively.

## 5. Analysis Methodology: DAE based PPTA

### 5.1 PPTA (Partial Periodic Trimming Algorithm)

If the installed rotor blades have the same configuration, helicopter states at a steady trim condition expects to have a partial periodic characteristic with the period of  $2\pi/n_b$ . The related partial periodicity condition for state variables can be represented with initial states  $\mathbf{x}(0)$  as equation (22) [2].

$$\mathbf{x}(2\pi/n_b) - \mathbf{P}\mathbf{x}(0) = \mathbf{0} \quad (22)$$

, where for the four bladed rotor

$$\mathbf{P} = \text{diag}(\mathbf{I}_9, \mathbf{P}_F, \mathbf{P}_L, \mathbf{I}_3, \mathbf{I}_5)$$

$$\mathbf{P}_F = \mathbf{P}_L = \text{diag}(\mathbf{P}_{FS}, \mathbf{P}_{FS})$$

$$\mathbf{P}_{FS} = \begin{bmatrix} \mathbf{0} & \mathbf{I}_3 \\ 1 & 0 \end{bmatrix}$$

Since a trim is an average feature of specific flight, its conditions can be satisfied with the average states  $\bar{\mathbf{x}}$  and constant control  $\mathbf{u}$  over a time period of  $2\pi/n_b$  as equation (23).

$$\mathbf{f}_{TRM}(\bar{\mathbf{x}}, \mathbf{u}) = \mathbf{f}_{TRM}(\bar{\mathbf{s}}) = \mathbf{0} \quad (23)$$

$$\text{, where } \bar{\mathbf{s}} = [\bar{\mathbf{x}} \quad \mathbf{u}]^T = \frac{n_b}{2\pi} \int_0^{2\pi/n_b} \mathbf{s}(\psi_R) d\psi_R$$

$$\mathbf{s} = [\mathbf{x} \quad \mathbf{u}]^T$$

PPTA is an iterative method to find the initial state  $\mathbf{x}(0)$  and control input  $\mathbf{u}$  which satisfies equations (22) and (23). The followings are the summary of PPTA iterative steps.

STEP 1: Specify initial conditions  $\mathbf{s}(0)$

STEP 2: Perturb initial conditions

$$\mathbf{s}_i(0) = \mathbf{s}(0) + \varepsilon_i \mathbf{e}_i(0) \quad (\varepsilon_0 = 0)$$

STEP 3: Time integration and calculate error vector (repeat STEP 2, 3 for all  $\mathbf{s}_i$ )

$$\mathbf{y}_i = \begin{bmatrix} \mathbf{x}(2\pi/n_b) \\ \boldsymbol{\delta} \end{bmatrix}_{\mathbf{s}_i(0)}, \quad \boldsymbol{\delta} = \mathbf{f}_{TRM}(\bar{\mathbf{x}}, \mathbf{u})$$

STEP 4: Calculate Jacobean Matrix  $\boldsymbol{\Phi}$

$$\boldsymbol{\Phi} = \frac{\partial \mathbf{y}}{\partial \mathbf{s}} = \begin{bmatrix} \boldsymbol{\Phi}_{11} - \mathbf{P} & \boldsymbol{\Phi}_{12} \\ \boldsymbol{\Phi}_{21} & \boldsymbol{\Phi}_{22} \end{bmatrix}$$

$$\boldsymbol{\Phi}_{11} = \frac{\partial \mathbf{x}(2\pi/n_b)}{\partial \mathbf{x}(0)} \quad \boldsymbol{\Phi}_{12} = \frac{\partial \mathbf{x}(2\pi/n_b)}{\partial \mathbf{u}}$$

$$\boldsymbol{\Phi}_{21} = \frac{\partial \boldsymbol{\delta}}{\partial \mathbf{x}(0)} \quad \boldsymbol{\Phi}_{22} = \frac{\partial \boldsymbol{\delta}}{\partial \mathbf{u}}$$

STEP 5: Newton Iterative Solution to get a new initial condition  $\mathbf{s}^{m+1}(0)$  (m: number of PPTA iteration, c: relaxation constant)

$$\mathbf{s}^{m+1}(0) = \mathbf{s}^m(0) - c \boldsymbol{\Phi}^{-1} \mathbf{E}^m$$

$$\mathbf{E}^m = \begin{bmatrix} \mathbf{x}(2\pi/n_b) - \mathbf{P}\mathbf{x}(0) \\ \boldsymbol{\delta} \end{bmatrix} = \mathbf{y}_0 - \begin{bmatrix} \mathbf{P}\mathbf{x}(0) \\ \boldsymbol{\delta} \end{bmatrix}$$

As shown in the above algorithm, time period of integration is reduced to  $2\pi/n_b$  rather than  $2\pi$  for normal periodic trimming algorithm. The computational time for time integration is greatly

reduced to the ratio of  $1/n_b$  per iteration and the number of a required trim iteration can become much less due to the reduced error with shorter time integration period.

## 5.2 DAE(Differential Algebraic Equation) Solver

DAE solver is a two step algorithm with a predictor step and a corrector step. The divided difference interpolation polynomials are used to predict the state variables and to transform its time derivatives as a function of state variables at  $n+1$  time step [7]. By using the notation of Reference 7 the  $k$ -th order DAE solver can be summarized as the following steps.

### I. Predictor Step ( $i = 0, 1, 2, \dots, k$ )

- (a)  $\omega_{n+1}^P(t_{n-i}) = x_{n-i}$
- (b)  $x_{n+1}^0 = \omega_{n+1}^P(t_{n+1})$
- (c)  $\dot{x}_{n+1}^0 = \dot{\omega}_{n+1}^P(t_{n+1})$

### II. Corrector Step: $1 \leq i \leq k$

- (d)  $\omega_{n+1}^C(t_{n+1} - ih_{n+1}) = \omega_{n+1}^P(t_{n+1} - ih_{n+1})$
- (e)  $\omega_{n+1}^C(t_{n+1}) = x_{n+1}$
- (f)  $\dot{\omega}_{n+1}^C(t_{n+1}) = \dot{x}_{n+1}$
- (g)  $f(\dot{\omega}_{n+1}^C(t_{n+1}), \omega_{n+1}^C(t_{n+1}), t_{n+1}) = 0$

, where  $h_{n+1} = t_{n+1} - t_n$

At the predictor step the predictor polynomial  $\omega_{n+1}^P$ , which satisfy (a), has been defined by using the previous calculation of state variables such as  $x_n, x_{n-1}, x_{n-2}, \dots$ . Then state variables at  $t_{n+1}$  can be predicted by using the equations of (b) and (c) and the predictor polynomial at time  $t$ .

$$\begin{aligned} \omega_{n+1}^P(t) &= x_n + (t - t_n)[x_n, x_{n-1}] \\ &+ (t - t_n)(t - t_{n-1})[x_n, x_{n-1}, x_{n-2}] \\ &+ \dots \\ &+ (t - t_n)(t - t_{n-1}) \dots (t - t_{n-k+1})[x_n, x_{n-1}, \dots, x_{n-k}] \end{aligned}$$

The corrector polynomial  $\omega_{n+1}^C$ , which satisfies (d) and (e), can be defined and by applying (f) the state derivative  $\dot{x}_{n+1}$  can be replaced with state variable  $x_{n+1}$ . Then the equation (g) is reduced to the system of algebraic equations as follow.

$$\dot{x}_{n+1} = \dot{x}_{n+1}^{(0)} - \frac{\alpha_s(x_{n+1} - x_{n+1}^{(0)})}{h_{n+1}}$$

$$\alpha_s = -\sum_{j=1}^k \frac{1}{j}$$

$$f\left(\dot{x}_{n+1}^{(0)} - \frac{\alpha_s(x_{n+1} - x_{n+1}^{(0)})}{h_{n+1}}, x_{n+1}, t_{n+1}\right) = 0 \quad (24)$$

Or  $f(\alpha x + \beta, x, t) = 0$  (without subscript  $n+1$ )

$$\text{, where } \alpha = -\frac{\alpha_s}{h_{n+1}}, \quad \beta = \dot{x}_{n+1}^{(0)} - \alpha x_{n+1}^{(0)}$$

By applying Newton iterative method, the following form of DAE solver can be obtained.

$$x^{(m+1)} = x^{(m)} - cG^{-1}f(\alpha x^{(m)} + \beta, x^{(m)}, t) = 0$$

$$\text{, where } G = \alpha \frac{\partial f}{\partial \dot{x}} + \frac{\partial f}{\partial x}$$

$c$  is under-relaxation constant

The Jacobean matrix  $G$  can be numerically calculated as follows

$$G_j \approx \frac{1}{2\Delta x_j} \left\{ f\left[\alpha(x + \Delta x_j e_j) + \beta, x + \Delta x_j e_j, t\right] - f\left[\alpha(x - \Delta x_j e_j) + \beta, x - \Delta x_j e_j, t\right] \right\}$$

## 5.3 Integration of DAE solver into PPTA

The accuracy and convergence of DAE solver for linear differential algebraic equation can be achieved with compatible initial conditions, which should satisfy the original DAE [4]. But DAE based PPTA cannot meet this compatibility condition due to state perturbations and state updates during iterative solution of PPTA. From the detail investigation, the reduction of DAE order at initial integration steps has been found to be an effective way for good convergence and the allowed maximum accuracy can be recovered by gradually increasing the order  $k$  of DAE solver according to the following logic.

$$k = \text{MIN}\left[\frac{m}{5} + 1, k_{\max}, n\right] \quad (25)$$

, where  $m$  Number of PPTA iteration  
 $k_{\max}$  Allowed maximum DAE order  
 $n$  Time step ( $n=1$  at  $\psi_R = 0$ )

The flight simulation from a calculated periodic trim condition can start with the allowed maximum DAE order.



## 6 APPLICATION

The present rotor aeromechanical equations and DAE based PPTA were applied to Bo-105 CBM (Common Baseline Model) helicopter which had been used by AGARD AGRTEUR AG06 working group during their collaborative research for helicopter flight mechanic analysis [6]. CBM helicopter has flapping dynamics with flap hinge spring and flap hinge damping. At the present analysis the dynamic inflow model (Ref 13) has been used rather than classical Glauert-trapezoidal inflow model in CBM. With the disc model for tail rotor, the flapping and the inflow of tail rotor have the forms of pure algebraic equation. But as already mentioned, the time integration by DAE solver can simultaneously process these algebraic equations with DAE for the dynamic equations of airframe, main rotor flapping and main rotor inflow.

The convergence history in section 6.1 has been calculated with;

- ✓ Azimuth element = 144 ( $\Delta\psi_R = 2.5$  Deg)
- ✓ Forward speed  $V_F = 250$  km/hr

If not specifically mentioned, the trim calculations have been obtained with the following baseline conditions.

- ✓ DAE order = 3<sup>rd</sup> order
- ✓ Azimuth element = 36 ( $\Delta\psi_R = 10$  Deg)
- ✓ Radial blade elements = 10

### 6.1 Convergence history

The convergent periodic trim history has been calculated at forward flight speed of  $V_F = 250$  km/hr. Fig. 3 shows the RMS value of the difference between two successive calculations of initial trim states. Around 20 iterations (5 rotor revolutions) are enough for the converged periodic trim calculation and the jumps in 5<sup>th</sup> and 10<sup>th</sup> iteration are occurred due to the stepwise increase in the order of DAE solver. The time history of states and pitch controls are shown in Fig.4, Fig.5 and Fig.6, which showed the nearly periodic properties after 2 rotor revolutions (8 PPTA iterations).

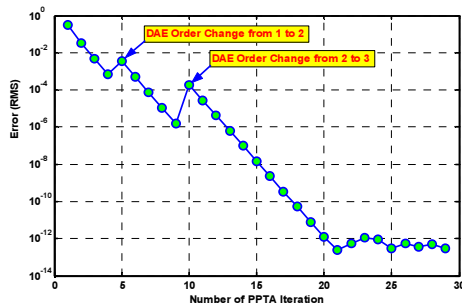


Fig. 3 Convergence History

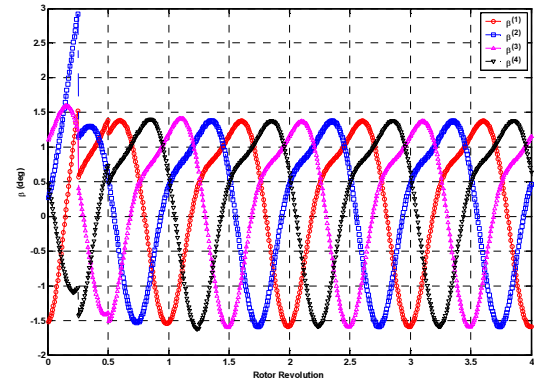


Fig. 4 History of Flap Response

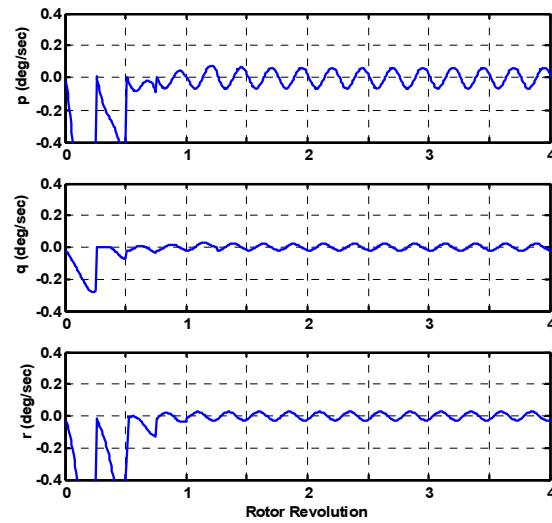


Fig. 5 History of Angular Response

### 6.2 Periodic Flap Response

The analysis conditions for good trim prediction have been deduced from the fully converged periodic flap solution with variations of the time step size, the number of radial blade elements and the desired order of DAE solver. The trim conditions were calculated for the forward flight speed of  $V_F = 250$  km/hr.

Effects of time step size (in azimuth angle) Fig. 7 shows the converged flap response with variation of time step size of  $\Delta\psi_R = 5, 10, 15$  and  $22.5$  deg (72 ~16 azimuth elements). The desired accuracy can be obtained if  $\Delta\psi_R \leq 10$  deg. Fig. 8 showed the partially enlarged view of flap response to see more detail difference.

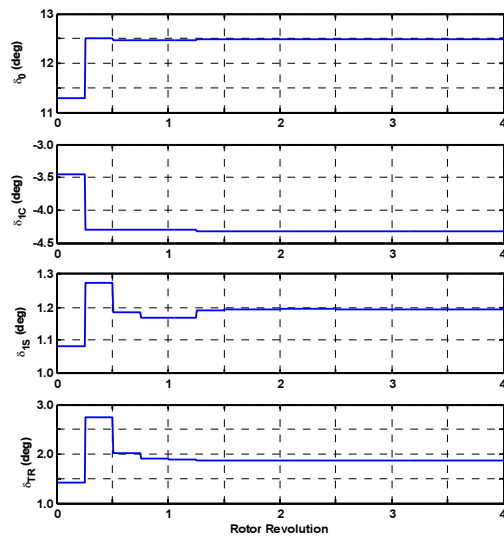


Fig. 6 Convergence History of Pitch Controls

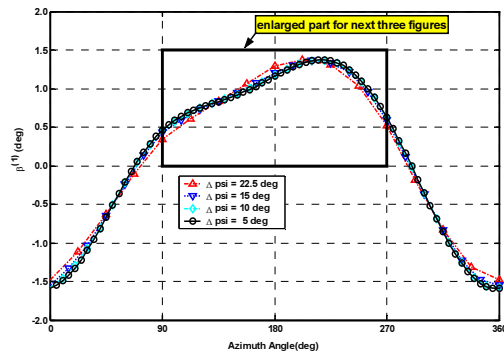


Fig 7 Converged Flap Response with time step size

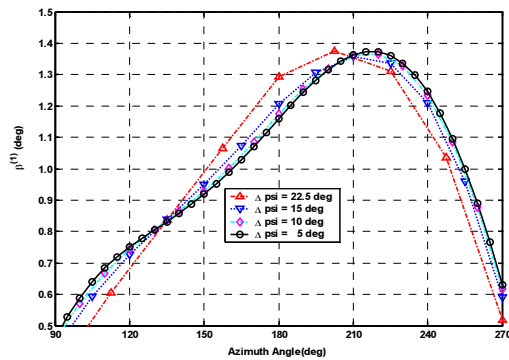


Fig 8 Enlarged View of Flap Response

Effects of the number of radial blade elements Fig. 9 shows the converged flap response with variation of the number of radial blade elements from 5 to 20. The analysis with more than 10 radial elements represents the nearly same results.

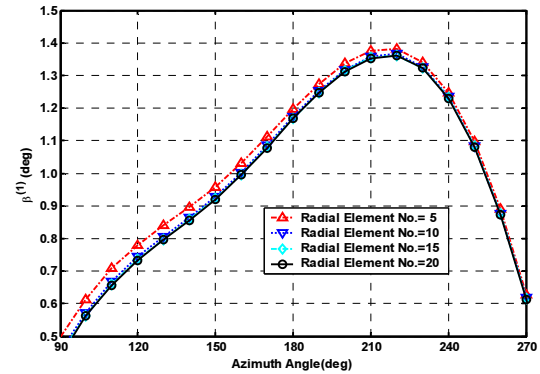


Fig.9 Flap Responses with Variation of the Number of Blade Radial Elements

Effects of the order of DAE solver Fig. 10 shows the effect of DAE order on the converged flap response. The analysis with DAE order equal to 1 differs from the other. So the good accuracy can be obtained with DAE order greater than or equal to 2.

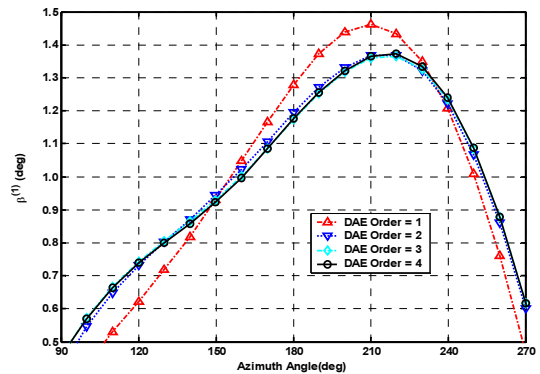


Fig.10 Flap Responses with Variation of DAE Order

### 6.3 Effects of Forward Speed on Trim Control

Fig.11, Fig.12 and Fig.13 show the blade pitch control inputs with variation of forward flight speed from 0 to 250 km/hr. The PPTA assumes the control inputs are constant even if the state variables should meet a partial periodicity condition given in equation (22). The effects of time step size, the number of blade radial elements and DAE order on the trim control inputs are negligible except a minor

difference in the lateral cyclic control  $\delta_{LC}$  of main rotor. As in the flap response the effect of DAE order is the greatest and DAE order greater than 2 is enough to get a good accuracy.

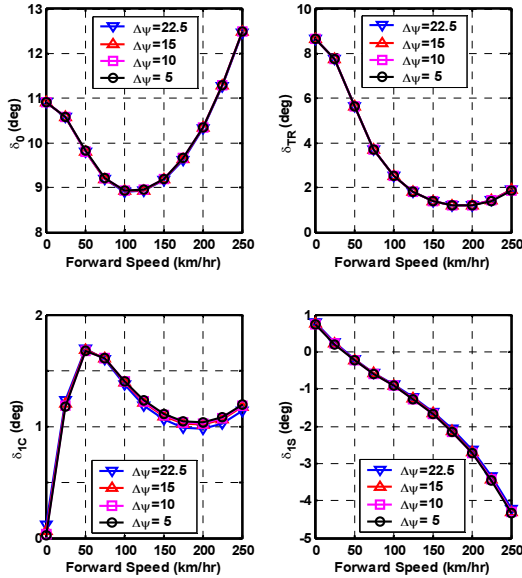


Fig.11 Trim Controls with Varying Time Step Size

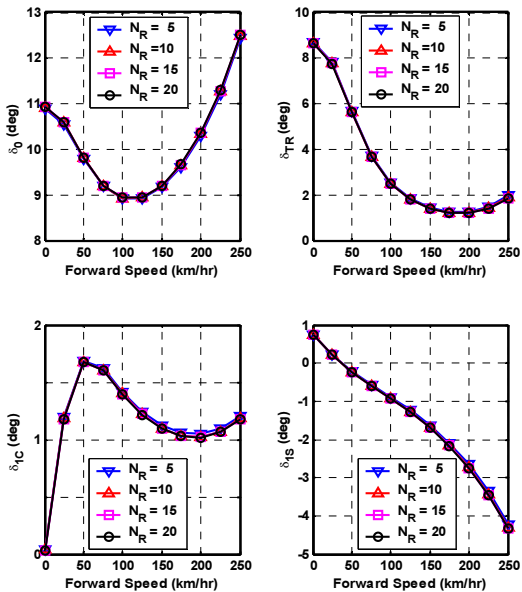


Fig.12 Trim Controls with Varying the Number of Blade Radial Elements

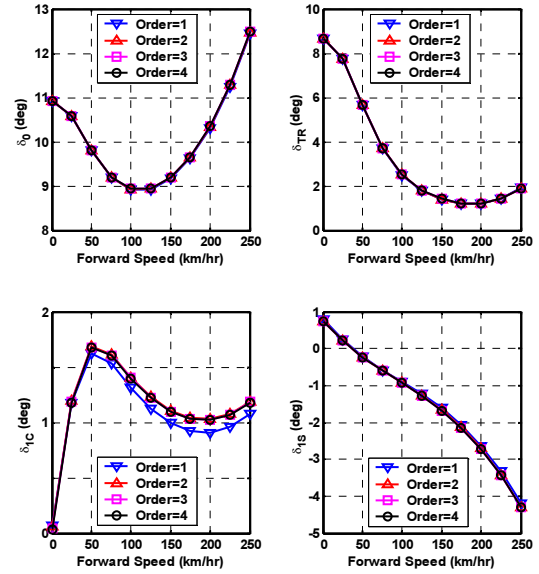
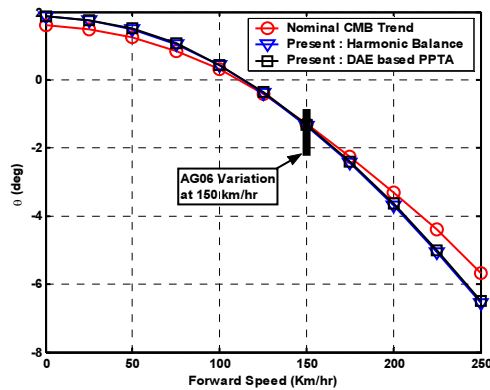


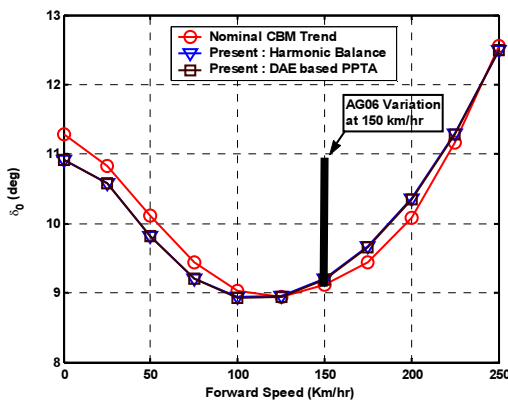
Fig.13 Trim Controls with Varying DAE Order

#### 6.4 Correlation with AGARD GARTEUR AG06 Results

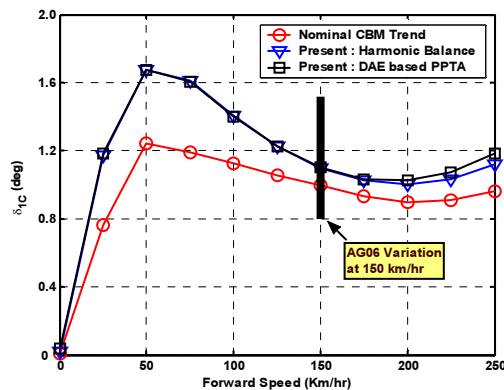
To show the accuracy of present algorithm, the calculated results are correlated with the results of AGARD GARTEUR AG06 (Ref 11). Two kinds of trim analysis methods have been applied to the present formulation of helicopter flight dynamic equations. One is the harmonic balance methods and the other is the DAE based PPTA. Because the trim states calculated by DAE based PPTA show the periodic characters, those are averaged over one rotor revolution for comparisons. Fig. 14 shows the airframe pitch angle and main rotor controls with variation of forward flight speed. The average trim states calculated by present DAE based PPTA are nearly same as the trim calculation by harmonic balance method. Also except the lateral cyclic control of main rotor the calculated results have shown good correlations with Nominal CBM Trends which are the averaged trim value over different participants in the AGARD GARTEUR AG06. To show the scatter in the trim results among AG06, the variations are presented at  $V_F = 150$  km/hr in the figure. The root cause of the lateral cyclic trim control has been already investigated in Ref 11.



(a) Airframe Pitch Angle



(b) Main Rotor Collective Pitch



(c) Main Rotor Lateral Cyclic Pitch

Fig. 14 Correlation with AGARD AG06 Results

The cyclic trim control calculated with dynamic inflow model rather than classical Glauert-trapezoidal inflow model has shown a clearer shape

of spoon which is similar to with flight test results (Ref 11). The present analysis with dynamic inflow has presented the same tendency.

## CONCLUSIONS

The present formulation for rotor dynamics and the periodic trim calculation with DAE based PPTA show the following key results.

1. The fully implicit formulation in this study can be easily modified for its application to any rotor with arbitrary hinge geometry and hinge sequence.
2. The DAE solver and PPTA have been successfully integrated by adjusting DAE order and the results show the fast convergence.
3. From the application to AGARD AG06 CBM helicopter, the accurate calculation can be obtained with (1) azimuth elements more than 36, (2) radial blade elements larger than 10 and (3) DAE order greater or equal to 2.
4. The calculated trim states and trim control inputs are well correlated with the results of AGARD GARTEUR AG06

## REFERENCES

1. Gareth D. Padfield, *Helicopter Flight Dynamics : The Theory and Application of Flying Qualities and Simulation Modeling*, Blackwell Science Ltd , 1996.
2. M. Hamers and W. von Gruhagen, "Dynamic Engine Model integrated in Helicopter Simulation", 23<sup>rd</sup> European Rotorcraft Forum Proceeding, 1997.
3. Robert T. N. Chen, "A Simplified Rotor System Mathematical Model for Piloted Flight Dynamics Simulation", NASA TP-78575, Nasa Ames, 1979.
4. R. Celi and P. P. Friedmann, "Rotor Blade Aeroelasticity in Forward Flight with an Implicit Aerodynamic Formulation", *AIAA Journal*, Vol.26, No.12, pp1425-1433, December, 1988.
5. R. Celi, "Effect of Hingeless Rotor Aeroelasticity on Helicopter Longitudinal Flight Dynamics", *Journal of American Helicopter Society*, pp35-43, January, 1991
6. R. Celi, "Rotor Blade Aeroelasticity in Forward Flight with an Implicit Structural Formulation", *AIAA Journal*, Vol.30, No.9, pp2274-2282, September, 1992.
7. K. E. Brenen, S. L. Campbell and L. R. Petzold, *Numerical Solution of Initial-Value Problems in Differential-Algebraic Equations*, Society for Industrial and Applied Mathematics, 1996.

8. R. Celi, "Implementation of Rotary-Wing Aeromechanical Problems with Differential-Algebraic Equation Solvers," 55th AHS Forum Proceeding, 1999.
9. J. Scott G. McVicar and Roy Bradley, "An Investigation into the Stability Characteristics of a Tilt-Rotor Configuration in Turning Flight Using Advanced Modeling and Fast Analysis Techniques," 22nd European Rotorcraft Forum, no.2, 1996, pp.73.1-73.211.
10. David A. Peters, "Fast Floquet Theory and Trim for Multi-Bladed Rotorcraft", 51th American Helicopter Society Forum Proceeding, 1995, pp444-459.
11. Gareth D. Padfield, et al, "Predicting Rotorcraft Flying Qualities through Simulation Modeling : A Review of Key Results From GARTEUR AG06," European Rotorcraft Forum, v.22, no.2, 1996, pp.71.1-71.14
12. B. Etkin, *Dynamics of Atmospheric Flight*, John Wiley & Sons, Inc. , 1972
13. David A. Peters and Ninh HAQuang, "Dynamic Inflow for Practical Applications", Journal of American Helicopter Society, October, 1988.